

# Semi-Perturbative Unification with extra vector-like families

Mar Bastero-Gil<sup>a</sup> and Biswajoy Brahmachari<sup>b</sup>

(a) Department of Physics  
University of Southampton  
Southampton SO17 1BJ, UK.

(b) Physics Department  
Indiana University  
Bloomington, IN 47406, USA.

## Abstract

We make a comprehensive analysis of an extended supersymmetric model (ESSM) obtained by adding a pair of vector-like families to the minimal supersymmetric standard model and having specific forms of  $5 \times 5$  fermion mass matrices. The two-loop Yukawa effects lead to an unified coupling  $\sim 0.2$  and unification scale  $\sim 10^{16.9}$  GeV. The renormalization effects of the extra vector-like generations on soft masses make the superparticle mass spectrum distinct from MSSM. This also has important effects on the charge and color breaking minima. We demonstrate that there exists minima of the Higgs potential which satisfies the mass of the Z boson but avoid electric charge and color breaking. Upper limit on the mass of the lightest Higgs from one-loop effective scalar potential is derived which reduces from MSSM.

# 1 Introduction

Seeking to achieve compatibility between low-energy data and string unification, the commonly accepted notion of a weak unified coupling  $\alpha_X = 0.04$ , based on the assumption of the MSSM spectrum has been questioned in an earlier work [1]. It was suggested in Ref [1] that the four dimensional unified string coupling should very likely have a semi-perturbative value ( $\sim 0.2$ - $0.3$  say), at the string unification scale, so that it may be large enough to stabilize the dilaton, but not so large as to disturb the coupling unification relations.

Bearing this in mind, as well as the fact that the MSSM unification scale  $M_X = 2 \times 10^{16}$  GeV [2], appears to be a factor of 20 smaller than the expected (one-loop level) string unification scale of  $(M_{st} \sim g_{st} 5.2 \times 10^{17}) GeV \sim 3.6 \times 10^{17}$  GeV [3] the consequences of a previously suggested extension [1] of the MSSM spectrum with regard to the issues of  $\alpha_X$  and  $M_X$ , mentioned above, were explored in Ref[1]. This extension, called as the **Extended Supersymmetric Standard Model (ESSM)**, assumes the standard model gauge symmetry below the unification scale, but extends the MSSM spectrum by adding to it two light vector like families  $Q_{L,R} = (U, D, N, E)_{L,R}$  and  $Q'_{L,R} = (U', D', N', E')_{L,R}$ , two Higgs singlets ( $H_S$  and  $H_\lambda$ ), and their SUSY partners, all at about 1 to a few TeV. The combined sets  $(Q_L|\overline{Q'})$  and  $(\overline{Q_R}|Q'_L)$  transform as 16 and  $\overline{16}$  of  $SO(10)$  respectively.

It has been noted sometime ago [5] that although precision measurements of the oblique electroweak parameters and of  $N_\nu$  disfavour a fourth chiral family, they are rather insensitive to an extra pair of vector like families. Thus vector like families (ie pairs of 16 and  $\overline{16}$ ), which

incidentally arise rather generically in string theories, may well exist in the TeV region, (but) not yet felt, even indirectly. Further more, it has also been observed [6] the existence of an extra pair of vector like family would enable one to obtain a simple understanding of the inter family mass hierarchy of the three chiral families via a see-saw mechanism for the down as well as the up sector.

In Ref [1], it was shown that such an extra pair of vector like families and thus ESSM provide some unique advantage over MSSM. They are as follows. (i) First, in one-loop, ESSM is guaranteed to preserve the success of MSSM as regards the approximate meeting of the three gauge couplings simply because the differences of the one-loop  $\beta$  function coefficients for the three couplings are independent of the number of generations (ignoring Yukawa couplings). (ii) While in one-loop, the extra pair of Vector-like families and their SUSY partners lead to the meeting of the three  $\alpha_i$ 's at the same position  $M_X$ , as does MSSM, they inevitably raise the slope of each  $\alpha_i$  and thereby raise the value of the unified coupling  $\alpha_X$  at  $M_X$ , compared to that for MSSM, just as desired. (iii) Once  $\alpha_X$  is raised, as it turns out to nearly  $0.2 - 0.3$  in one loop (see below), two-loop effects involving contributions of gauge couplings to their self-evolutions naturally become important, especially near  $M_X$ . These two-loop gauge coupling contributions, which raise the slopes of the  $\alpha_i$ 's, together with the softening effects of the Yukawa couplings, which do just the opposite, were studied in detail in Ref [1], In these studies, smoothed out exact threshold functions [7] as opposed to  $\theta$  functions were used, allowing for a wide range of variation of the ESSM spectrum in the region  $m_Z \rightarrow 5$  TeV. The evolution of the Yukawa couplings of the model associated with

the see-saw mass matrix was, however, studied, for simplicity, only in one-loop, which was inserted into the evolution of the gauge couplings. All the off-diagonal Yukawa couplings of the third chiral family with the two vector-like families as well as the self couplings of the vector-like families (See Yukawa coupling matrix later) were taken to be large ( $\sim 1-2$ ) in all four sectors (up, down, charged lepton and neutrinos), so that they approach their fixed point values at the electroweak scale. The combined effects of the two-loop gauge contributions, together with one-loop Yukawa contributions and smoothed threshold functions, exhibited the following desirable features [1]. (a) Even with the inclusion of the two-loop effects, the three couplings (still) met, remarkably enough to a degree better than one-loop, for a wide range of variation of the spectrum, and that too with a higher  $\alpha_X \sim (0.2-0.3)$ , as well as higher  $M_X \approx 10^{17}$  GeV (compare with  $\alpha_X \approx 0.04$  and  $M_X \sim 2 \times 10^{16}$ ) GeV for MSSM, just as desired. The value of  $M_X$  for ESSM is certainly closer to the expected string-scale than that for MSSM. The remaining gap of a factor of 5 or so between  $M_X$  and  $M_{st}$  in ESSM may be in part due to the increased importance of the two-loop string threshold effects, corresponding to a semi-perturbative value of  $\alpha_X$ , which could lead to a significant correction to a one-loop formula for  $M_{st}$ , and in part due to three and higher loop effects (see remarks in [1]). (b) The added desirable feature is that in ESSM the couplings meet for typically low values of  $\alpha_3(m_Z)|_{\overline{MS}}^{ESSM} \sim 0.120-0.124$ , which are in accord with the observed value of  $\alpha_3(m_Z)|_{\overline{MS}}^{obs} = 0.117 \pm 0.005$ . By contrast, for MSSM, barring GUT-threshold and Planck scale effects, one typically needs higher values of  $\alpha_3(m_Z)|_{\overline{MS}}^{MSSM} > 0.125$  if  $m_{\tilde{q}} < 1$  TeV and  $M_{1/2} < 500$  GeV [8], which are not in such good agreement with observation.

In summary, ESSM which was studied in the approximation of 2-loop evolution of the gauge couplings, including 1-loop evolution of the Yukawa couplings, exhibits many desirable features. Apart from providing a simple explanation of the inter-family mass-hierarchy, it provides unification with a higher ( $\alpha_X \sim 0.2 - 0.3$ ), a higher ( $M_X \sim 10^{17}$ ) GeV and a lower  $\alpha_s(m_Z)$  compared to MSSM, as desired.

Given these promising features to serve as motivation for further study of ESSM, the purpose of this note is to explore the issue of unification in ESSM further, by improving the approximation of Ref. [1], especially by including 2-loop evolution of the Yukawa couplings. It is worth noting that the 3-loop evolution of the gauge couplings in ESSM, including contributions from gauge interactions only, has been studied partially in the mean time in Ref [8]. It is encouraging that this study showed essential stability of the results of Ref. [1], except for some increase in  $M_X$  in some cases relative to the 2-loop result of Ref. [1]. The main reason to study especially the 2-loop evolution of the Yukawa couplings for ESSM is that there are many large Yukawa couplings for ESSM - some 20 in number as opposed to 1 or 2 for MSSM - which are large at  $M_X$  (See definition of Yukawa coupling matrix later). At this point, it is important to recall that the Yukawa contributions, whose evolutions were treated in one-loop, exhibited marked beneficial effects for ESSM, in damping the growth of gauge couplings, especially in the region closer to  $M_X$ . This damping in fact played a crucial role in leading to unification of the gauge couplings with a semi-perturbative value of  $\alpha_X \sim 0.2 - 0.3$ , as opposed to non-perturbative values of  $O(1)$  [16], and that too with a relatively low value of  $\alpha_3(m_Z)$ , in accord with observation. Now, considering that the

gauge, as well as, some 20 Yukawa couplings are relatively large at  $M_X$  for ESSM (i.e.  $\alpha_i \sim \alpha_{yuk}^j \sim 0.2 - 0.3$  at  $M_X$ ), which influence each others evolutions, one would apriori expect that the combined 2-loop contributions of gauge as well as Yukawa interactions to the evolutions of the Yukawa couplings would be quite significant [17]<sup>1</sup>, relative to the 1-loop contributions, especially near  $M_X$ . It is thus imperative to check whether the inclusion of these 2-loop contributions to the evolution of the Yukawa couplings would preserve, improve or alter adversely the desirable features as regards unification of couplings as obtained in [1].

## 2 Evolution of couplings at two-loops

### 2.1 Definitions

We perform a 2-loop analysis of the RGEs (renormalization group equations) of the gauge couplings including the effects of the third generation Yukawa couplings at two-loop, and carefully taking into account the threshold effects due to the spread of the superpartner masses and the masses of the particles in the vector-like families. Furthermore we use mass dependent running of the gauge couplings (see Eqn.(2)), or equivalently the effective couplings formalism which guarantees a smooth crossover at the threshold of each individual particle. The 2-loop RGEs for the Yukawa couplings are given in the Appendix, and those

---

<sup>1</sup>Naively, one would estimate the ratio of 2-loop versus 1-loop contributions to the  $\beta$  functions for the Yukawa couplings to be  $\sim [(g^2 \text{ or } h^2)/4\pi](4\pi)^{-1} C$ , where the coefficient  $C$  are typically large. Taking a collective representative value of  $C \sim 10 - 30$ , would suggest that the ratio of relative contributions can be about 25 to 75 % near  $M_X$ , for  $g^2/4\pi \sim h^2/4\pi \sim 0.25$  (say). We, of-course, calculate these contributions exactly.

for the gauge couplings are,

$$\frac{d\alpha_i^{-1}}{dt} = -\frac{b_i}{2\pi} - \sum_j \frac{b_{ij}}{8\pi^2} \alpha_j + \sum_k \frac{a_i^{(k)}}{8\pi^2} Y_k, \quad (1)$$

with  $t = \ln \mu$  and  $Y_k = h_k^2/(4\pi)$ . The coefficients  $b_i$ ,  $b_{ij}$  and  $a_i^{(k)}$  are listed in the Appendix.

When working with a mass dependent subtraction procedure, these coefficients depend on the scale  $\mu$  through the ratios  $m_k/\mu$ , where  $m_k$  is any mass running inside the loop. Integrating Eq. (1) we would obtain the analytical expressions for the effective couplings, which at 1-loop order are given by,

$$\alpha_i^{-1}(\mu) = \alpha_i^{-1}(m_Z) + \sum_k \frac{b_i^k}{2\pi} (F_k(m_k/\mu) - F_k(m_k/m_Z)) . \quad (2)$$

The threshold function  $F_k(m_k/\mu)$  has the value  $\ln m_k/\mu$  in the limit  $m_k/\mu \rightarrow 0$ . Therefore, when all the masses are well below the scale  $m_Z < \mu$  we recover the familiar one-loop expression,

$$\alpha_i^{-1}(\mu) = \alpha_i^{-1}(m_Z) - \frac{b_i}{2\pi} \ln \left( \frac{\mu}{m_Z} \right). \quad (3)$$

On the other hand,  $F_k(m_k/\mu)$  vanishes in the limit  $m_k/\mu \rightarrow \infty$ , giving the familiar decoupling of heavy masses from the running of the couplings. Thereby a smooth threshold crossing with the variation of  $\mu$  is obtained as stated above. The two-loop parts of the beta functions  $b_{ij}$  and  $a_i^{(k)}$  are matched at each threshold using step-function approximation (see Appendix). The details of our procedure to determine the masses of the superpartners and a discussion on radiative electroweak breaking in this model is given in the following section.

Near the unification scale, the Yukawa coupling matrix for the third and the heavy

vector-like generations (denoted for simplicity as  $16$  and  $\overline{16}$ ) have the form,

$$h_{f,c}^{(o)} = \begin{matrix} & 16_3 & \mathbf{16} & \overline{\mathbf{16}} \\ \begin{matrix} 16_3 \\ \mathbf{16} \\ \overline{\mathbf{16}} \end{matrix} & \begin{pmatrix} 0 & x_f H_f & y_f H_S \\ y'_c H_S & 0 & z_f H_\lambda \\ x'_c H_f & z'_c H_\lambda & 0 \end{pmatrix} \end{matrix} . \quad (4)$$

The couplings  $x_f, x'_c$  ( $y_f, y'_c$ ) are the interaction between the chiral and vector-like generations with the doublet scalars  $H_1, H_2$  (singlet scalar  $H_S$ ) whereas  $z_f, z'_c$  give the interactions between the vector-like generations and the singlet  $H_\lambda$ . Note that this is a formal representation of the Yukawa matrix. A detailed definition of Yukawa matrices is given in the Appendix. While evolving the couplings from the unification scale down to the electroweak scale the vector-like generations get decoupled, consequently the Yukawa matrices get rotated which projects the effective third generation Yukawa couplings ( $h_t, h_b$  and  $h_\tau$ ) at  $m_Z$ . Hence the RGE for the Yukawa couplings are integrated in a top-down approach in the ranges  $M_X \rightarrow M_Q \rightarrow M_L \rightarrow m_Z$ , with the boundary conditions,

$$\begin{aligned} h_t(M_Q) &= \left( \frac{x'_u y_u}{z_u} + \frac{x_u y'_q}{z'_q} \right) \frac{v_S}{v_\lambda} \Big|_{M_Q}, \\ h_b(M_Q) &= \left( \frac{x'_d y_d}{z_d} + \frac{x_d y'_q}{z'_q} \right) \frac{v_S}{v_\lambda} \Big|_{M_Q}, \\ h_\tau(M_L) &= \left( \frac{x'_e y_e}{z_e} + \frac{x_e y'_l}{z'_l} \right) \frac{v_S}{v_\lambda} \Big|_{M_L}, \end{aligned} \quad (5)$$

at the vector-like thresholds. Here  $M_Q$  and  $M_L$  denote the masses of quark and leptonic members of the extra generations, and  $v_S = \langle H_S \rangle$ ,  $v_\lambda = \langle H_\lambda \rangle$ . Assuming the Yukawa couplings to be large at the unification scale ( $h_i(M_X) = \sqrt{4\pi}$ ), we evolve them to the scale  $m_Z$ , so that they approach their fixed point near  $m_Z$ . In order to prevent a too low value of



$h_t(m_Z)$ , and consequently a too low prediction for the top mass, we fix  $v_S/v_\lambda \simeq 0.5$  in this section.

We impose the unification condition at  $M_X$ ,  $\alpha_1(M_X) = \alpha_2(M_X) = \alpha_3(M_X) = \alpha_X$ . After evolving the gauge couplings down to  $m_Z$  we use the central values values of  $\sin^2 \theta_w = 0.2319$  and  $\alpha_{em}^{-1}(m_Z) = 127.9$  to fit  $M_X$  and  $\alpha_X$ . Once  $M_X$  and  $\alpha_X$  are known (which depend on the mass spectrum of the vector-like as well as superpartners) we predict the QCD coupling  $\alpha_3(m_Z)$  using 2-loop RGE. In order to compare the values of  $\alpha_i(m_Z)$  with the experimental values, we have consistently changed the effective couplings to their  $\overline{MS}$  values. Typically, the  $U(1)$  and  $SU(2)$  effective couplings are only of order 1% larger than the  $\overline{MS}$  couplings, but  $\alpha_3(m_Z)$  can be 5–8% larger, depending on the SUSY spectrum considered.

## 2.2 Comparing one and two loop results

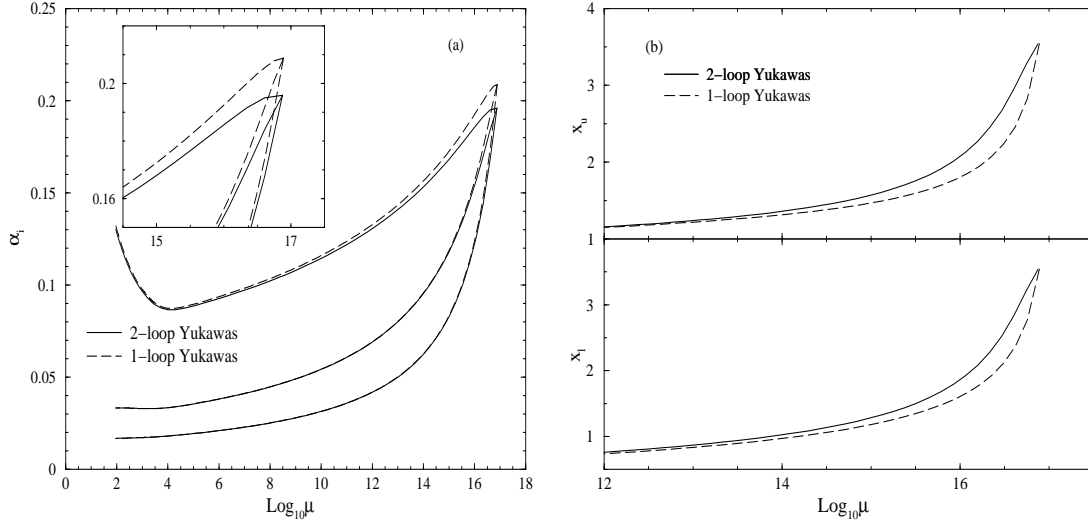


Figure 1: (1.a) Running of the gauge couplings when the Yukawa couplings are taken at one loop (dashed line) and at two-loop (solid line). (1.b) Running of the Yukawa couplings at one loop (dashed line) and two loops (solid line).  $M_2 = 90$  GeV,  $\tilde{m}_q = \tilde{m}_h = 1$  TeV,  $M_Q = 3$  TeV.

In Fig. (1.a) the evolution of the effective gauge couplings with the Yukawa couplings calculated at 1-loop and 2-loops are compared. In this example we have fixed the mass spectrum<sup>2</sup> taken  $M_Q = 3$  TeV, the wino mass  $M_2 = 90$  GeV, and the squark mass  $\tilde{m}_{qL}$  and higgsino mass  $\tilde{m}_h$  at 1 TeV; the heavier Higgses are also taken at 1 TeV while keeping the lightest Higgs mass at 90 GeV. For the sake of simplicity, when computing the threshold functions we neglect the mixing between charginos and higgsinos as well as between squarks/sleptons left and right. For the vector-like generations we assume the mass pattern  $M_Q \sim \tilde{m}_Q$ ,  $M_L \sim \tilde{m}_L$ ,  $M_Q \approx 3M_L$ , where the factor of 3 corresponds primarily to QCD renormalization effects.

We first notice that in the high energy region the 2-loop Yukawas are larger than the 1-loop Yukawas (see Fig. (1.b)). For the gauge couplings this has the effect of flattening their curves near the unification scale, specially in the case of the QCD coupling. Due to the large number of Yukawa couplings in the model, its contribution in Eq. (1) becomes comparable to the pure gauge contribution and may almost cancel it, and this effect will last slightly longer when the Yukawas couplings are also integrated at 2-loop order. Nevertheless, the Yukawa couplings approach very quickly their infrared fixed point and for them the distinction between 1-loop and 2-loop becomes negligible in the low energy region. However, from the point of view of gauge coupling unification the overall effect would be a small decrease of the values of  $\alpha_X$  and  $\alpha_3(m_Z)$ , but an increase of  $M_X$ .

Next question to ask is how much these predictions vary when the scale  $M_Q$  is varied.

---

<sup>2</sup>These are the values we will use to compute the threshold functions in the evolution of the effective couplings hereafter, unless other values be given explicitly.

Intuitively it is clear that we should recover the MSSM results at the limit  $M_Q \rightarrow M_X$ . In Fig. (2) we have plotted the predictions when varying  $M_Q$  including the results with 1-loop Yukawas (curves labelled (a)) and 2-loop Yukawas (curves labelled (b)). In these figures we have also considered a higher gaugino mass  $M_2 = 200$  GeV. Once  $\tilde{m}_{q_L}$  and  $M_2$  are fixed so is  $M_0$  and  $M_{1/2}$  at the unification scale (Fig. (3)). These are the values used to compute the RGE predictions in Figure (2).

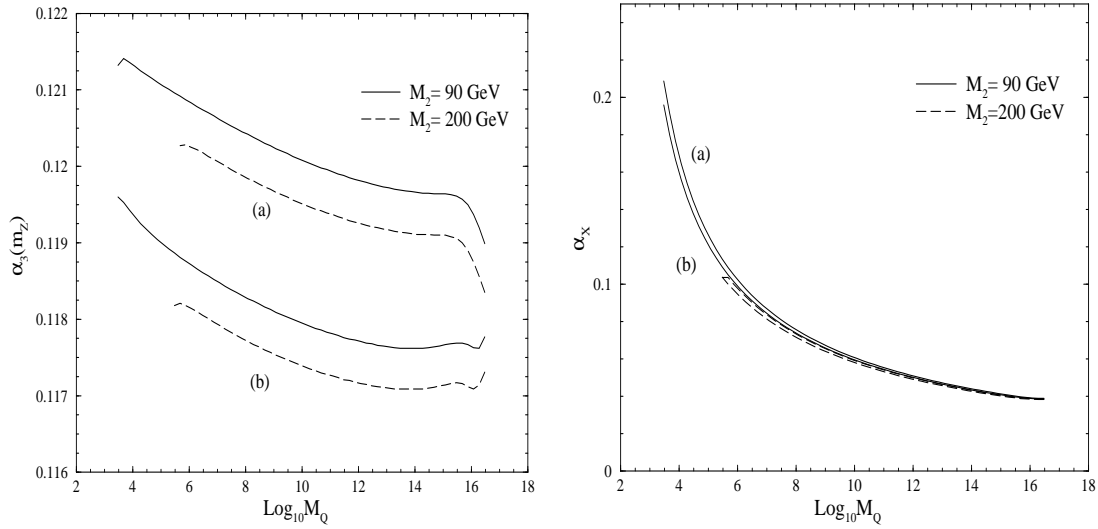


Figure 2: The predicted values of  $\alpha_3(m_Z)$  and  $\alpha_X$  varying  $M_Q$ . The solid and dashed lines are for different  $M_2$  as given in the legend. Curves labelled (a) are obtained with the Yukawas integrated at 1-loop, whereas those labelled (b) include the Yukawas at 2-loop.

The plotted value of  $\alpha_3(m_Z)$  is their  $\overline{MS}$  value. When  $M_Q$  is near the TeV range, the three gauge couplings are non-asymptotically free for most of the range of integration, and they merge together at a larger value of  $\alpha_X$  compared with the MSSM prediction. When  $M_Q$  increases asymptotic non-free behavior is lost and we recover MSSM results.

Having fixed the ratio  $v_S/v_\lambda \approx 0.5$ , and giving as input  $m_\tau = 1.777$  GeV, we have checked that the predictions for top quark mass and the bottom quark mass are consistent with their

experimental current values. We have:  $m_t^{pole} \approx 165 - 180$  GeV,  $m_b(m_b) \approx 6.2 - 4.4$  GeV, for  $M_Q$  in the range 3 TeV- $10^{16}$  GeV, and the value of  $\tan\beta \sim m_t/m_b$  will range approximately from 35 to 60.

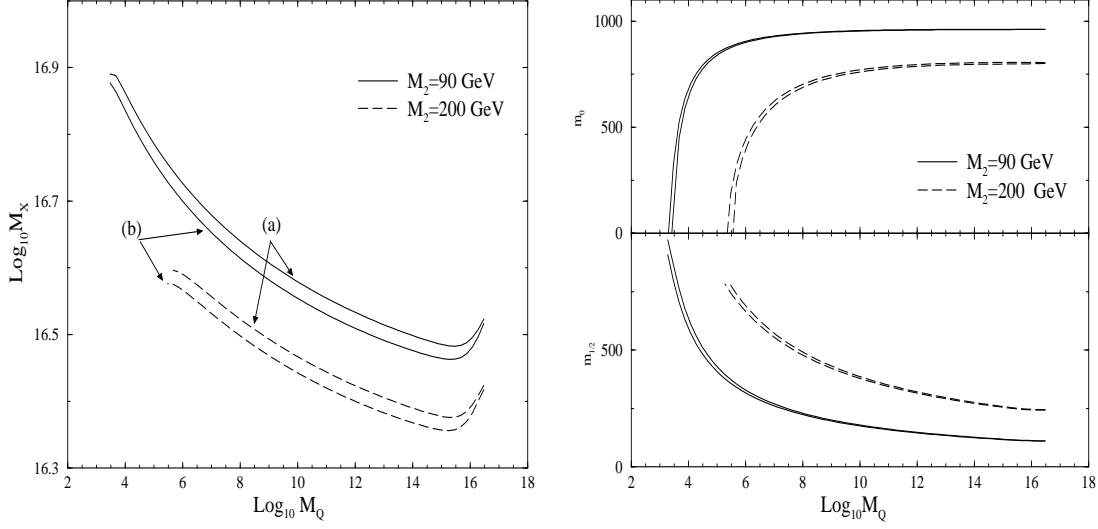


Figure 3: Left plot: The predicted values of  $M_X$ ; labels (a) and (b) mean Yukawa coupling integrated at 1-loop or 2-loop respectively. Right plot: The fitted values of  $M_0$  and  $M_{1/2}$  requiring that the highest chargino mass  $M_{1/2}$  is 90 GeV and first and second generation squark masses are at 1 TeV.

### 2.3 Problems in the fixed-point scenario.

It is clear that the most interesting situation from the point of view of semiperturbative unification would be to have the extra vector-like generations around a scale of a few TeV. However, the mass of the extra vector-like generations can be related to the effective  $\mu$  parameter needed to get electroweak symmetry breaking. Due to this, a simple numerical estimation shows that the scenario with *all* the Yukawas in the model at their infrared fixed point is excluded if  $M_Q \sim O(\text{TeV})$ .

The superpotential for the scalar Higgses is given by:

$$W = k_1 H_1 H_2 H_\lambda + \frac{k_2}{3} H_\lambda^3 + \frac{k_3}{3} H_S^3 \quad (6)$$

The singlet  $H_S$  plays no role in the EWSB, and mainly gets decoupled from the other scalars. But the singlet  $H_\lambda$  plays the role of the field  $N$  in the Next-to-Minimal Supersymmetric Standard Model (NMSSM) [9, 10, 11], and EWSB is driven when it gets a vev. The effective  $\mu$  parameter is defined by:

$$\mu \equiv k_1 v_{H_\lambda} , \quad (7)$$

with the coupling  $k_1$  evaluated at the weak scale, and typically we expect  $\mu \approx 1$  TeV. The vectorlike masses are obtained by diagonalising the matrix given in Eq. (4), but in a first approximation they are given by,

$$M_{U1} \simeq M_{D1} \simeq z'_q(M_Q) v_\lambda, \quad M_{U2} \simeq z'_u(M_Q) v_\lambda, \quad M_{D2} \simeq z'_d(M_Q) v_\lambda, \quad (8)$$

and similarly for the heavy leptons, with the ratio  $z'_q(M_Q)/z'_l(M_L) \approx 3$  due to renormalization effects. For an extra vector scale of the order of some TeVs, we have the near-infrared fixed points,

$$z'_q(M_Q) \simeq 0.73, \quad z_u(M_Q) \simeq 0.56, \quad z_D(M_Q) \simeq 0.53, \quad (9)$$

and  $k_1 \simeq 0.01$ . In this situation we expect  $v_\lambda = \mu/k_1 \approx O(100 \text{ TeV})$ , and thus we would have  $M_Q \approx O(50 \text{ TeV})$ , much larger than the initially assumed value for this scale. Therefore, if we want to consider smaller values of the vectorlike scale, the initial values of the couplings  $z_f$  and  $z'_c$  at the GUT scale have to be reduced in order to fit the input value for  $M_Q$ .

In the next section we will see that large Yukawa couplings at the GUT scale has a

significant effect on the susy spectrum. Notice that the effect of large Yukawa couplings is to diminish the s-particle masses. This in turn will favour the presence of charge and/or color breaking minima driven by trilinear couplings, even when the traditional constraint [10, 12],

$$|A_{ijk}|^2 < 3(m_i^2 + m_j^2 + m_k^2), \quad (10)$$

is satisfied. In fact, when *all* the Yukawa couplings are at the infrared fixed point region, a closer examination of the minimisation conditions of the scalar potential [13] shows that there is always a charge and color breaking minima deeper than the electroweak symmetry breaking one, for any value of  $M_Q$ . Consequently the Yukawa couplings have to be diminished at the gut scale to recover a global charge and color conserving minima.

## 3 Higgs and S-particle spectrum

### 3.1 Soft mass evolution

Assuming the universality of soft supersymmetry breaking terms at the GUT scale, the SUSY spectrum at the weak scale is given in terms of following parameters at the GUT scale apart from all Yukawa couplings presented in the previous sections:

$$\text{gaugino mass} = M_{1/2} \ ; \ \text{scalar mass} = M_0 \ ; \ \text{trilinear coupling} = A_0, \quad (11)$$

The gaugino masses  $M_i$  are calculated integrating the 2-loop RGE,

$$\frac{dM_i/\alpha_i}{dt} = \sum_j \frac{b_{ij}}{8\pi^2} \alpha_j^2 \frac{M_j}{\alpha_j} \quad (12)$$

The squark and slepton masses of the first and second generation (neglecting small D-term contributions) are calculated from the 1-loop expression:

$$\frac{d\tilde{m}_a^2}{d\ln\mu} = -\frac{1}{2\pi} \sum_i 4C_2(R_a)\alpha_i M_i^2, \quad (13)$$

where  $C_2(R_a) = (N^2 - 1)/2N$  for the fundamental representation of  $SU(N)$ . When calculating the squark and slepton masses of the third generation we have properly taken into account the effects of the related Yukawa couplings. We have taken  $\sqrt{4\pi}$  as the initial value at the GUT scale for the Yukawa couplings related to  $h_t(m_t)$ , so that  $h_t(m_t)$  is at the infrared fixed point.

The 1-loop RGE Eq. (13) can be easily integrated numerically. It is convenient to represent them after integration as,

$$\tilde{m}_a^2 = M_0^2 + c_a M_{1/2}^2, \quad (14)$$

where the constants  $c_a$  depend on the values of the gauge couplings and their  $\beta$ -functions, and thus implicitly on the vector-like scale  $M_Q$ . Compared to MSSM, in the ESSM we obtain an enhancement of the squark and slepton spectrum for fixed gaugino masses, as was noticed in Ref. [8]. This is clearer if we rewrite Eq. (14) in term of the wino mass  $M_2$ ,

$$\tilde{m}_a^2 = M_0^2 + \hat{c}_a M_2, \quad (15)$$

where the values of  $\hat{c}_a$  are much larger than expected in MSSM. This can be seen in the MSSM limit  $M_Q \geq 10^{16.5}$  GeV in Table 1.

---

We quote the coefficients for the left handed squarks<sup>3</sup>, sleptons left and right, and the

<sup>3</sup>Those for the right handed squarks, up and down, are roughly the same as  $\hat{c}_Q$ . In fact, in the numerical

$M_Q$	$\hat{c}_Q$	$\hat{c}_L$	$\hat{c}_R$	$M_{1/2}/M_2$	$M_3/M_2$	$M_2/M_1$
$3\text{ TeV}$	110.2	21.2	8.8	8.8	3.8	1.6
$300\text{ TeV}$	27.3	4.7	1.8	4.0	3.9	1.8
$10^{10}\text{ GeV}$	10.7	1.2	0.4	1.9	4.0	1.9
$10^{16.5}\text{ GeV}$	9.3	0.8	0.2	1.2	4.0	1.9
<i>MSSM</i>	9.3	0.8	0.2	1.2	4.0	1.9

Table 1: Coefficients  $\hat{c}_a$  for the left-handed squarks, left and right handed sleptons masses of the first and second generation.

ratios of the gaugino mass parameters, for different values of  $M_Q$ . Here we have still taken the initial values of all Yukawa couplings at the largest possible value for the sake of illustration. Later on we will fix the fermion masses and Yukawa couplings exactly. For low values of  $M_Q$  (order some TeVs) the squark and slepton masses of the first and second generation are dominated by the gaugino contribution. Even if we assume the wino to be light (on the border of the experimental lower limit), the squark masses are pushed up to the TeV range, the left-handed slepton mass is larger than the gluino mass  $M_3$ , and the right-handed slepton mass is roughly of the same order as  $M_3$ . On the other hand, as  $M_Q$  increases we tend to recover the MSSM limit where light gaugino masses but large squark masses imply a large value of  $M_0$ , as can be seen in Fig. (3). The ratio  $\frac{M_3}{M_2} \simeq 4$  is practically independent of  $M_Q$ . Thus we observe that in ESSM the superpartner spectrum is considerably different from MSSM due to the renormalization effects of the extra vector-like generations.

---

calculations of the effective couplings we have assumed degeneracy of left and right handed squarks, and both are taken to be  $\tilde{m}_q$ .



### 3.2 Tree level Higgs potential

As mentioned above, the Higgs sector of the ESSM resembles that of the Next-to-Minimal Supersymmetric Standard Model (NMSSM) with the vev of  $H_\lambda$  generating the effective  $\mu$  and  $B$  parameters at the weak scale:

$$\mu \equiv k_1 v_\lambda, \quad (16)$$

$$B \equiv k_2 v_\lambda + A_1. \quad (17)$$

The couplings  $k_1$ ,  $k_2$  and  $A_1$  (the trilinear coupling of  $k_1$ ) are evaluated at the weak scale. As in the NMSSM, the minimization conditions of the potential for the real components of scalars  $H_1$ ,  $H_2$  look like those of the MSSM, whilst the value of  $v_\lambda = \langle H_\lambda \rangle$  has to satisfy the extra condition:

$$\sin 2\beta = 2v_\lambda \frac{m_{H_\lambda}^2 + k_2 A_2 v_\lambda + k_1^2 v^2 + 2k_2^2 v_\lambda^2}{k_1 A_1 v^2 + 2k_1 k_2 v^2 v_\lambda}. \quad (18)$$

As usual, we have defined  $\tan \beta = v_2/v_1$  and  $v^2 = v_1^2 + v_2^2 = (175 \text{ GeV})^2$ . Now, for a given value of  $\tan \beta$  and  $k_1$  we can fit the appropriate values of  $k_2$  and  $A_i$  at the GUT scale, i.e., the universal trilinear coupling  $A_0$ . Once  $A_0$  is known, the effective  $\mu$  and  $B$  parameters are computed as displayed in Fig. (4). The value of  $\mu$  is roughly constant and of order the TeV scale, whereas the  $B$  parameter decreases with  $\tan \beta$ . We have fixed  $k_1(M_X) = \sqrt{(4\pi)}$  for simplicity, and typically  $k_2(M_X) < k_1(M_X)$  is the favoured parameter space in this case.

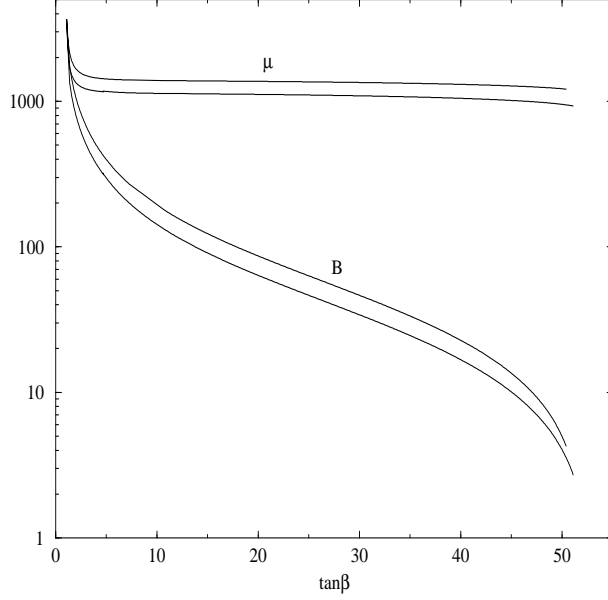


Figure 4: Values of the effective parameters  $\mu \equiv k_1(m_Z)v_\lambda$  and  $B \equiv k_2(m_Z)v_\lambda + A_1$  which gives rise to the correct  $m_Z$  after the radiative electroweak breaking. For each parameter, the lower curve correspond to  $M_0 = 0$ , and the upper curve to  $M_0 = 800$  GeV.

### 3.3 SUSY spectrum and radiative electroweak breaking

We note that in Fig. (2) we did not take into account the constraints from electroweak symmetry breaking (EWSB); we only displayed how the predictions vary when changing the extra vector scale  $M_Q$ . All the Yukawas were taken as  $(\sqrt{4\pi})$  at the unification scale, so that they approach their infrared fixed point at low energy. However, we have seen that such scenario cannot lead to the correct electroweak breaking minima when  $M_Q$  is only a few TeV. Then, we have to reduce at least the initial values of the couplings  $z_f$  and  $z'_c$  accordingly to our choice of the vector-like scale,  $M_Q = 3$  TeV.

In addition, the fixed point scenario always leads to a large value of  $\tan \beta$ . If we want to consider smaller values of  $\tan \beta$  the initial values for the Yukawas related with the bottom-

tau sector (  $x_f, x'_f$  ) should be also lowered. Therefore, in this section we will take  $\tan \beta$  as an input free parameter, and fit the Yukawa couplings such that they reproduce the experimental values of  $m_b(m_b) = 4.4$  GeV and  $m_\tau = 1.777$  GeV, while taking into account electroweak symmetry breaking.

	$\tan \beta = 5$	$\tan \beta = 30$	$\tan \beta = 50$
$v_\lambda/v_S$	0.325	0.317	0.255
$x_d(M_X), x_\tau(M_x)$	0.013, 0.029	0.096, 0.212	0.449, 0.908
$z_q(M_X), z_q(M_Q)$	0.133, 0.351	0.131, 0.343	0.086, 0.253
$z_u(M_X), z_u(M_Q)$	0.355, 0.621	0.338, 0.604	0.207, 0.469
$z_d(M_X), z_d(M_Q)$	0.218, 0.621	0.214, 0.604	0.155, 0.469
$k_2(M_X)$	0.932	0.940	0.297
$k_1(m_Z), k_2(m_Z)$	0.242, 0.158	0.220, 0.172	0.149, 0.113
$\hat{\alpha}_3$	0.124	0.123	0.120
$M_X$	16.94	16.93	16.88
$\alpha_X$	0.252	0.247	0.226

Table 2: Values of Yukawa couplings and the ratio  $v_\lambda/v_S$  needed to fit the fermion masses:  $M_Q = 3$  TeV,  $m_t = 175$  GeV,  $m_b = 4.4$  GeV,  $m_\tau = 1.7$  GeV. The prediction for  $\hat{\alpha}_3$ ,  $M_X$  and  $\alpha_X$  is also included.

In table 2 are given some of the values for the Yukawa couplings, and the corresponding prediction of  $\alpha_3$ ,  $M_X$  and  $\alpha_X$ . We have taken the following boundary conditions at the GUT scale:

$$\begin{aligned}
x_f &= x'_f, \quad y_f = z_f, \\
z'_q &= z'_l, \quad z_u = z_\nu, \quad z_d = z_e.
\end{aligned} \tag{19}$$

The remaining Yukawas not included in the table are taken at  $\sqrt{(4\pi)}$  at the unification scale. As expected, the prediction for  $\hat{\alpha}_3(m_Z)$  and  $\alpha_X$  decrease ( a 3% and 10% respectively) when increasing  $\tan \beta$ ; for large values of  $\tan \beta$  the Yukawa couplings related to the bottom and

tau sector are allowed to be larger and the model approaches the scenario given in section 2.

Having set the procedure to fix the various parameters of the model at the GUT scale, we can obtain now the SUSY mass spectrum predicted: Higgses (including the mixing between the standard doublets and the singlet  $H_\lambda$ ), squarks and sleptons, charginos, neutralinos and gluino. The specimen values with the variation with  $\tan \beta$  are given in table 3. In the first rows are given the mass parameters needed to obtain the spectrum. We have taken  $M_0 = 0$  to keep the first and second generation squark masses as low as possible; but even when  $M_0 = 0$ , these masses are in the TeV range due to large renormalization effect of the gauge couplings. The constraint of having EWSB demands an effective  $\mu$  parameter in the TeV range. With  $\mu \approx 1$  TeV and the low values of  $M_2$  and  $M_1$ , the gaugino-higgsino mixing is almost negligible, and the heavier chargino and neutralinos are predominantly higgsinos. In fact the heaviest neutralino is predominantly a singlino. Therefore, the spectrum obtained is consistent with our initial assumption of neglecting the mixings and having a higgsino mass of order of 1 TeV, and with the assumptions for the Higgs sector.

The same feature of small mixing is present in the scalar Higg sector between the doublets and the singlet. Due to the large value of  $\mu$ , the Higgs masses coming mainly from the doublets satisfy:

$$m_{S1} \ll m_{S2} \simeq m_{a1} \simeq m_{H^\pm} . \quad (20)$$

Notice that the lightest (tree-level) Higg mass quoted in table 3 is too low to be compatible with the current experimental lower bound of 95 GeV. The correct values of the Higgs masses

$m_i(\text{GeV})$	$\tan \beta = 5$	$\tan \beta = 30$	$\tan \beta = 50$
$M_0, M_{1/2}$	0, 1115	0, 1083	0, 952
$A_0$	-2768	-1922	-1800
$v_\lambda$	4828	4964	6389
$\mu \equiv k_1(m_Z)v_\lambda$	1169	1091	953
$B \equiv k_2(m_Z)v_\lambda + A_1(m_Z)$	297	34	4
$m_{S_1}$	64	73	81
$m_{S_2}, m_{S_3}$	1342, 1425	1057, 1490	439, 1171
$m_{a_1}, m_{a_2}$	1351, 958	1051, 1458	436, 1455
$m_{H^\pm}$	1345	1057	441
$\tilde{m}_{q_i}, i = 1, 2$	1185	1157	1042
$\tilde{m}_{l_i}, i = 1, 2$	536	522	466
$\tilde{m}_{\tau_i}, i = 1, 2$	355	345	305
$\tilde{m}_{t_1}, \tilde{m}_{t_2}$	653, 974	721, 879	680, 750
$\tilde{m}_{b_1}, \tilde{m}_{b_2}$	913, 1074	840, 984	617, 816
$\tilde{m}_\nu$	634	610	538
$\tilde{m}_{\tau_1}, \tilde{m}_{\tau_2}$	355, 645	265, 624	204, 568
$\tilde{m}_{\chi_1^\pm}, \tilde{m}_{\chi_2^\pm}$	87, 1175	89, 1097	89, 960
$\tilde{m}_{\chi_1^0}, \tilde{m}_{\chi_2^0}$	56, 90	58, 90	58, 92
$\tilde{m}_{\chi_3^0}, \tilde{m}_{\chi_4^0}$	957, 957	1094, 1094	1168, 1174
$\tilde{m}_{\chi_5^0}$	1530	1710	1441
$M_3$	357	355	348

Table 3: SUSY mass spectrum in the ESSM for the case of study,  $M_Q = 3$  TeV,  $M_2 = 90$  GeV. The values of the mass parameters at the GUT scale, and the derived effective parameters at the weak scale are also included. The Higg masses are tree-level masses.

are obtained once radiative corrections to the effective Higgs potential are included.

### 3.4 One loop effective potential

It is well known that radiative corrections coming from the one-loop effective potential can give an important contribution to the masses [14]. These corrections for the case of the MSSM plus a singlet have been calculated elsewhere [15], being the dominant one that due to loops of the top and stops. In particular, an upper bound can be obtained using the fact

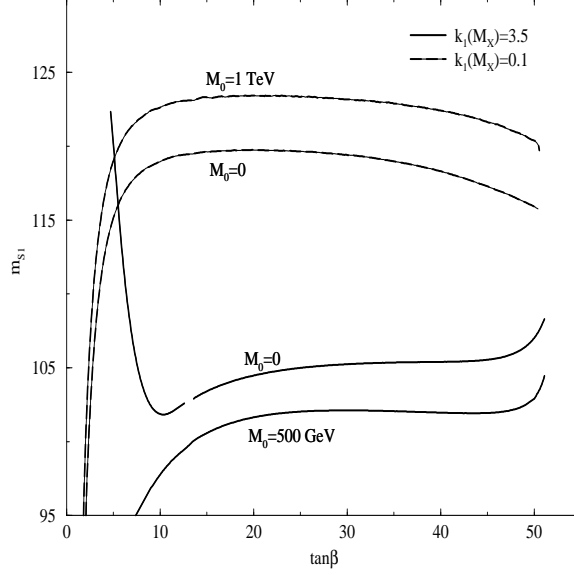


Figure 5: The lightest Higgs mass including one-loop radiative corrections due to quark-squarks and lepton-sleptons loops. Solid (dashed) lines are computed by taking various values of  $k_1$ ,  $M_Q = 3$  TeV  $M_2 = 90$  GeV.

that the lightest Higgs mass must be less or equal to the minimum eigenvalue of the  $2 \times 2$  CP-even Higgs mass matrix for the doublets, given by,

$$m_{S1}^2 \leq m_Z^2 (\cos^2 2\beta + \frac{k_1^2 v^4}{m_Z^4} \sin^2 2\beta) + \frac{3}{8\pi^2} h_t^2 m_t^2 \sin^2 \beta \left( \ln \frac{\tilde{m}_{t1}^2 \tilde{m}_{t2}^2}{m_t^4} + \frac{(A_t + \mu \cot \beta)^2}{(\tilde{m}_{t1}^2 - \tilde{m}_{t2}^2)} \ln \frac{\tilde{m}_{t1}^2}{\tilde{m}_{t2}^2} + \dots \right), \quad (21)$$

and then,

$$m_{S1} \leq 120 \text{ GeV}, \quad (22)$$

for the spectrum given in table 3. The upper bound is saturated when the mixing between the doublets and the singlet is negligible, that is, for small values of the coupling  $k_1$ . In table 4 are given the numerical values of the one-loop corrected Higgs masses including top-stops, bottom-sbottoms and tau-staus effects. We give the Higgs spectrum obtained when

	$k_1(M_X) = 3.5$			$k_1(M_X) = 0.1$		
$m_i(GeV)$	$\tan \beta = 5$	$\tan \beta = 30$	$\tan \beta = 50$	$\tan \beta = 5$	$\tan \beta = 30$	$\tan \beta = 50$
$m_{S_1}$	120	105	107	115	119	116
$m_{S_2}, m_{S_3}$	1061, 1423	1227, 1490	961, 1171	1342, 3950	1176, 2124	847, 1439
$m_{a_1}, m_{a_2}$	1090, 934	1219, 1461	959, 1455	1342, 6840	1176, 3678	847, 2493
$m_{H^\pm}$	1061	1190	799	1344	1147	698

Table 4: Higg masses including one-loop radiative corrections.  $M_Q = 3$  TeV,  $M_2 = 90$  GeV,  $M_0 = 0$ .

$k_1(M_X) = \sqrt{4\pi}$  and  $k_1(M_X) = 0.1$  for comparison. Lowering the value of the Yukawa  $k_1$  affects the Higgs sector, but it leaves the rest of the spectrum practically untouched. The values given in table 4 are for the case  $M_0 = 0$ . Larger values of  $M_0$  will imply a general increase in the susy spectrum, and in principle we can also rise in this way the value of  $m_{S_1}$ . However this is not the case if we take  $k_1$  to be large (see Fig. (5), and in this situation the lightest Higg mass decreases with  $M_0$ . This effect has nothing to do with the one-loop effective potential corrections to the masses, but with the running of the Higg sector parameters (Yukawas and masses), and the fact that the mixing with the singlet increase. The overall effect is that tree-level potential lightest mass is smaller, and radiative corrections are not enough to overcome this effect. In fact, as we increase  $M_0$  low values of  $\tan \beta$  will not be compatible with the current experimental lower bound on  $m_{S_1}$ . When  $M_0 \geq 800$  GeV we have  $m_{S_1} < 95$  GeV for any value of  $\tan \beta$ . We remark that the constraint on  $M_0$  is lost by reducing the value of  $k_1$ , that is, in the limit in which the singlet is effectively decoupled from the Higgs doublets.

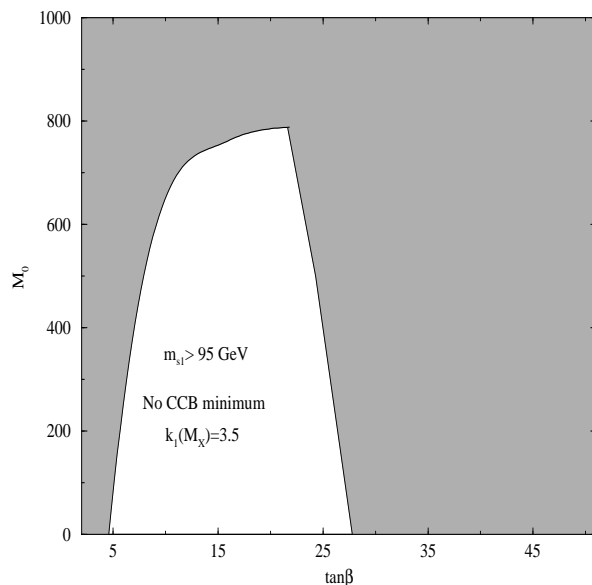


Figure 6: Taking  $M_{1/2} = 90$  GeV, we have plotted the parameter space which gives rise to charge and color conserving minima in the  $M_0 - \tan \beta$  with  $k_1^2(M_X) = 4\pi$ . When all Yukawas are at the fixed point the required  $\tan \beta$  is typically  $m_t/m_b \sim 40 - 60$ . Note that there is no charge and color conserving solutions in this case.

### 3.5 Charge and Color breaking revisited

Stronger constraints in the parameter space at the GUT scale are obtained demanding that no charge and color breaking (CCB) minima of the scalar potential is present at low energy. Large Yukawa couplings may drive the soft supersymmetry breaking soft mass terms to negative values, provided the superparticles whose masses are being considered interacts via the Yukawa coupling under consideration. For example a large top Yukawa coupling drives the Higgs masses to negative values triggering radiative electroweak breaking. ESSM has a number of large Yukawa couplings at the GUT scale, hence there is a possibility that their renormalization effects may lead to masses of superparticles with  $SU(2)_L$  and color quantum numbers to values which may trigger charge and color breaking. This will be essentially the



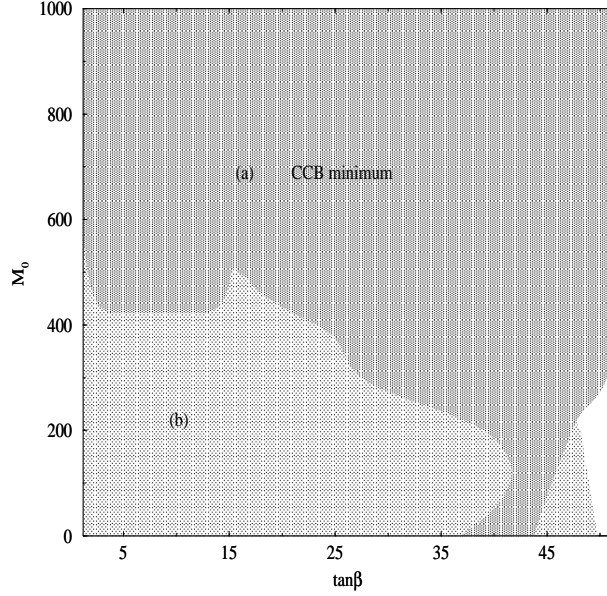


Figure 7: Taking  $M_{1/2} = 90$  GeV, we have plotted the parameter space which gives rise to charge and color conserving minima in the  $M_0 - \tan \beta$  plane. In this case we have taken  $k_1 = 0.1$ . Region (a) correspond to the standard CCB constraint, and region (b) correspond charge breaking due to a negative vector-like slepton squared mass. Most of the plane is excluded.

situation when  $M_0$  and/or  $\tan \beta$  are large. In order to get the constraint in the plane  $M_0$ - $\tan \beta$  we check that for each set of parameters corresponding to an EWSB minimum there is not a deeper charge or color breaking minimum<sup>4</sup> The allowed parameter space obtained when  $k_1(M_X) = \sqrt{(4\pi)}$  is given in Fig. (6), where we have also included the constraint  $m_{S1} \geq 95$  GeV. The later condition forbids low values of  $\tan \beta$ , whilst the CCB constraint excludes large values of  $\tan \beta$ .

As mentioned above, the constraint on the low values of  $\tan \beta$  can be relaxed reducing  $k_1(M_X)$ , although the maximum allowed value for  $M_0$  would get reduced by the CCB

---

<sup>4</sup>This condition does not exclude the existence of CCB minima, it only ensures that the global minimum is the EWSB minimum.

constraint (see Fig. (7)). Reducing  $k_1$  will also have the marginal effect of allowing slightly larger values for the couplings  $z_f, z'_f$ , which turns to be enough to directly affect the masses of the vector-like slepton masses. The latter are given by diagonalising squared mass matrices similar to those for the third generation squarks and slepton, for example:

$$\mathcal{M}^2(E'_L, E'_R) = \begin{pmatrix} \tilde{m}_{E_L}^2 + z_E^2 v_\lambda^2 & z_E(k_1 v_1 v_2 - k_2 v_\lambda^2 + A_N v_\lambda) \\ z_N(k_1 v_1 v_2 - k_2 v_\lambda^2 + A_E v_\lambda) & \tilde{m}_{E_R}^2 + z_E^2 v_\lambda^2 \end{pmatrix}, \quad (23)$$

where  $\tilde{m}_{E_i}^2$  are the soft running masses. For a vectorlike scale  $M_L \approx M_Q/3 \approx 1$  TeV, the off-diagonal terms in the above mass matrix can compete with the diagonal ones, increasing the splitting between the eigenvalues and even rendering one of them negative. This would be the situation for most of the parameter space when  $k_1(M_X) = 0.1$  as shown in Fig. (7). A neutral slepton squared mass becoming negative may only indicate that this neutral slepton would also get a vev, and may affect consequently the values of the other vevs in the model. But a negative charged slepton squared mass would imply a new source of electric charge breaking minima in the model, and has to be avoided. Due to this, the only parameter space left available in this case is a small corner for large values of  $\tan \beta$ . We remark that there is not such constraint due to the vector-like masses for larger values of  $k_1$  (smaller values of  $z_f$ ).

## 4 Conclusion

We question the commonly accepted notion of a unified gauge coupling  $\alpha_X \approx 0.04$ . If the Minimal Supersymmetric Standard Model (MSSM) is extended by including two vector like families (ESSM) the couplings grow stronger than the low energy ones due to the renormal-

ization effects of the extra matter and unify at a semi-perturbative value of around 0.2. This is in fact the only extension of MSSM containing complete families of quarks and leptons that is permitted by measurements of the oblique electroweak parameters on one hand and renormalization group analysis on the other hand. The former restricts one to add only vector like families whereas the latter states that no more than one pair of families can be added. In ESSM, as an example, the weak  $SU(2)$  coupling grows by a factor of six at the unification scale compared to its weak-scale value (see Fig. 1.a). Thus it can be conjectured that the four dimensional string coupling may have a similar intermediate value which is large enough to stabilize the dilaton problem. Furthermore, ESSM has a unique pattern of the Yukawa matrices which is motivated by preon theories. The extra vector like matter and normal matter has off diagonal Yukawa couplings whereas the normal three generations do not have Yukawa couplings among them at-all. This leads to a see-saw like picture of fermion masses; where after the decoupling of heavy matter a hierarchical mass pattern of standard fermions emerge. If we fix all the Yukawa couplings to be large at the unification scale, unique predictions of the low energy fermion masses emerge as the Yukawa couplings approach their quasi-infrared fixed points. On the contrary the renormalization effects of these relatively large Yukawa couplings have non-trivial effects on the unification of gauge couplings. Keeping this in mind we have performed the renormalization group evolution of the gauge couplings taking into account the Yukawa effects at the two-loop order. If we assume the universality of the soft SUSY-breaking parameters at the unification scale, renormalization group evolutions enable us to determine the SUSY spectrum at low energy. Note that due to the presence of the heavy generations the renormalization of the s-fermion mass

parameters are considerably different from that of MSSM. This makes ESSM from MSSM from the point of view of collider searches. The first and second generation squarks do not have large Yukawa renormalization hence they experience pronounced QCD renormalization which make them heavy (see fig (3.b)), without the need of a large initial value  $M_0$ .

A further question will be to get the correct radiative electroweak breaking. We have pointed out that the mass of the vector-like generations is linked to electroweak symmetry breaking by the approximate relation  $M_Q \approx (z_q/k_1)\mu$ . In particular, an electroweak symmetry breaking minimum which fits the mass of the Z boson exactly cannot be obtained in the infrared fixed-point Yukawa scenario if  $M_Q$  is below  $O(100\text{ TeV})$ . Moreover, the fixed-point scenario (large  $\tan\beta$ ) suffers from the presence of charge and color breaking minima. On the other hand, a global charge and color conserving minima can be obtained giving up the assumption of *all* Yukawas at their fixed point.

## Acknowledgement

We thank K. S. Babu, J. C. Pati and A. Rasin for discussions and critical appreciations.

## 5 Appendix

## 5.1 Yukawa evolution coefficients

The RGE for the Yukawa couplings (at any order) are given by the general expression,

$$(16\pi^2)\frac{dh_{ij}^m}{dt} = h_{ik}^m(\gamma_L)_j^k + (\gamma_R)_k^i h_{kj}^m + h_{ij}^m \gamma_{H_m}, \quad (24)$$

where  $h_{ij}^m$  is the Yukawa coupling for the right-handed field  $R_i$ , the left-handed field  $L_j$  and the scalar  $H_m$ . The functions  $\gamma_A$  are the anomalous dimensions for the superfield  $A$  [18]. To set the notation, we define  $h_{ij}^m$  as the Yukawa coupling when all the superfields enter in the vertex, and  $h_{ij}^{m\dagger}$  when they leave.

We have used the 2-loop anomalous dimensions to evaluate the expression in Eqn(24) which can be written as,

$$(\gamma_A)_j^i = (\gamma_A^{(1)})_j^i + \frac{1}{16\pi^2}(\gamma_A^{(2)})_j^i \quad (25)$$

Where the component one-loop and two-loop parts are given by the expressions,

$$(\gamma_A^{(1)})_j^i = h_{ik}^m h_{kj}^{m\dagger} - 2g_a^2 C_2(R_a) \delta_{ij}, \quad (26)$$

$$(\gamma_A^{(2)})_j^i = -\left(h_{ik}^m (\gamma_B^{(1)})_l^k h_{lj}^{m\dagger} + h_{ik}^m \gamma_{H_m}^{(1)} h_{kj}^{m\dagger}\right) + 2b_a C_2(R_a) g_a^4 \delta_{ij} - 2(\gamma_A^{(1)})_j^i C_2(R_a) g_a^2, \quad (27)$$

being  $g_a$  the gauge coupling,  $b_a$  the 1-loop gauge  $\beta$ -function and  $C_2(R_a)$  the quadratic Casimir for the  $R_a$  dimensional irreducible representation. In the ESSM, the anomalous dimensions can be further expanded in terms of four Yukawa coupling matrices  $h_f^m$  related to the four Higgs bosons (at the GUT scale they can be thought of a 10 and two singlets of SO(10))  $m = H_1, H_2, H_S, H_\lambda$ , with  $f = u, d, l, \nu$ . For example, the up sector Yukawa matrix can

be re-expanded in terms of the individual matrices

$$h_u^{H_2} = \begin{pmatrix} 0 & x_u & 0 \\ x'_q & 0 & 0 \\ 0 & 0 & 0 \end{pmatrix}, \quad (28)$$

$$h_u^{H_S} = \begin{pmatrix} 0 & 0 & y_u \\ 0 & 0 & 0 \\ y'_q/\sqrt{2} & 0 & 0 \end{pmatrix}, \quad (29)$$

$$h_u^{H_\lambda} = \begin{pmatrix} 0 & 0 & 0 \\ 0 & 0 & z_u \\ 0 & z'_q/\sqrt{2} & 0 \end{pmatrix}, \quad (30)$$

and similarly for the down-quark sector and the leptonic sector. The normalization factor  $\sqrt{2}$  is introduced to avoid overcounting when summing over  $f = u, d$  or  $f = l, \nu$ .

The 1-loop anomalous dimensions for the quark sector are given below. Those for the fields which transform as 16 of  $SO(10)$  (third generation and the set  $(Q_L|\bar{Q}')$ ) are expressed in terms of  $2 \times 2$  matrices, whereas the set transforming as  $\bar{16}$  is evaluated separately:

$$(\gamma_u^{(1)})_{ij} = 2(h_u^{H_2} h_u^{H_2^\dagger})_{ij} + (h_u^{H_S} h_u^{H_S^\dagger})_{ij} + (h_u^{H_\lambda} h_u^{H_\lambda^\dagger})_{ij} - \left( \frac{8}{15} g_1^2 + \frac{8}{3} g_3^2 \right) \delta_{ij}, \quad (31)$$

$$(\gamma_d^{(1)})_{ij} = 2(h_d^{H_1} h_d^{H_1^\dagger})_{ij} + (h_d^{H_S} h_d^{H_S^\dagger})_{ij} + (h_d^{H_\lambda} h_d^{H_\lambda^\dagger})_{ij} - \left( \frac{2}{15} g_1^2 + \frac{8}{3} g_3^2 \right) \delta_{ij}, \quad (32)$$

$$\begin{aligned} (\gamma_q^{(1)})_{ij} &= (h_u^{H_2^\dagger} h_u^{H_2})_{ij} + (h_d^{H_1^\dagger} h_d^{H_1})_{ij} + (h_u^{H_S^\dagger} h_u^{H_S})_{ij} + (h_d^{H_S^\dagger} h_d^{H_S})_{ij} + (h_u^{H_\lambda^\dagger} h_u^{H_\lambda})_{ij} \\ &\quad + (h_d^{H_\lambda^\dagger} h_d^{H_\lambda})_{ij} - \left( \frac{1}{30} g_1^2 + \frac{3}{2} g_2^2 + \frac{8}{3} g_3^2 \right) \delta_{ij}, \end{aligned} \quad (33)$$

$$i, j = 1, 2$$

$$\gamma_U^{(1)} = (h_u^{H_\lambda^\dagger} h_u^{H_\lambda})_{(3,3)} + (h_u^{H_S^\dagger} h_u^{H_S})_{(3,3)} - \frac{8}{15} g_1^2 - \frac{8}{3} g_3^2, \quad (34)$$

$$\gamma_D^{(1)} = (h_d^{H_\lambda^\dagger} h_d^{H_\lambda})_{(3,3)} + (h_d^{H_S^\dagger} h_d^{H_S})_{(3,3)} - \frac{2}{15} g_1^2 - \frac{8}{3} g_3^2, \quad (35)$$

$$\begin{aligned}
\gamma_{\bar{Q}}^{(1)} &= (h_u^{H_\lambda} h_u^{H_\lambda^\dagger})_{(3,3)} + (h_d^{H_\lambda} h_d^{H_\lambda^\dagger})_{(3,3)} + (h_u^{H_S} h_u^{H_S^\dagger})_{(3,3)} + (h_d^{H_S} h_d^{H_S^\dagger})_{(3,3)} \\
&\quad - \frac{1}{30} g_1^2 - \frac{3}{2} g_2^2 - \frac{8}{3} g_3^2,
\end{aligned} \tag{36}$$

In order to express the two-loop anomalous dimensions in matrix form, it is useful to arrange the  $2 \times 2$  matrices with the  $\bar{16}$  anomalous dimension in  $3 \times 3$  matrices as follow:

$$\gamma_{\bar{U}}^{(1)} = \begin{pmatrix} (\gamma_{\bar{u}}^{(1)})_{ij} & 0 \\ 0 & \gamma_{\bar{Q}}^{(1)} \end{pmatrix}, \tag{37}$$

$$\gamma_{\bar{D}}^{(1)} = \begin{pmatrix} (\gamma_{\bar{d}}^{(1)})_{ij} & 0 \\ 0 & \gamma_{\bar{Q}}^{(1)} \end{pmatrix}, \tag{38}$$

$$\gamma_{Q_u}^{(1)} = \begin{pmatrix} (\gamma_q^{(1)})_{ij} & 0 \\ 0 & \gamma_U^{(1)} \end{pmatrix}, \tag{39}$$

$$\gamma_{Q_d}^{(1)} = \begin{pmatrix} (\gamma_q^{(1)})_{ij} & 0 \\ 0 & \gamma_D^{(1)} \end{pmatrix}. \tag{40}$$

Using these matrices, the 2-loop contribution to the anomalous dimensions for the quark sector are given by,

$$\begin{aligned}
(\gamma_{\bar{u}}^{(2)})_{ij} &= - \left( 2h_u^{H_2} (\gamma_{Q_u}^{(1)} + \gamma_{H_2}^{(1)}) h_u^{H_2^\dagger} + h_u^{H_S} (\gamma_{Q_u}^{(1)} + \gamma_{H_S}^{(1)}) h_u^{H_S^\dagger} + h_u^{H_\lambda} (\gamma_{Q_u}^{(1)} + \gamma_{H_\lambda}^{(1)}) h_u^{H_\lambda^\dagger} \right)_{ij} \\
&\quad - \left( \frac{8}{15} g_1^2 + \frac{8}{3} g_3^2 \right) (\gamma_{\bar{u}}^{(1)})_{ij} + \left( \frac{8}{15} b_1 g_1^4 + \frac{8}{3} b_3 g_3^4 \right) \delta_{ij}
\end{aligned} \tag{41}$$

$$\begin{aligned}
(\gamma_{\bar{d}}^{(2)})_{ij} &= - \left( 2h_d^{H_1} (\gamma_{Q_d}^{(1)} + \gamma_{H_1}^{(1)}) h_d^{H_1^\dagger} + h_d^{H_S} (\gamma_{Q_d}^{(1)} + \gamma_{H_S}^{(1)}) h_d^{H_S^\dagger} + h_d^{H_\lambda} (\gamma_{Q_d}^{(1)} + \gamma_{H_\lambda}^{(1)}) h_d^{H_\lambda^\dagger} \right)_{ij} \\
&\quad - \left( \frac{2}{15} g_1^2 + \frac{8}{3} g_3^2 \right) (\gamma_{\bar{d}}^{(1)})_{ij} + \left( \frac{2}{15} b_1 g_1^4 + \frac{8}{3} b_3 g_3^4 \right) \delta_{ij},
\end{aligned} \tag{42}$$

$$\begin{aligned}
(\gamma_q^{(2)})_{ij} &= (h_u^{H_2^\dagger} (\gamma_{\bar{U}}^{(1)} + \gamma_{H_2}^{(1)}) h_u^{H_2} + h_d^{H_1^\dagger} (\gamma_{\bar{D}}^{(1)} + \gamma_{H_1}^{(1)}) h_d^{H_1} + h_u^{H_S^\dagger} (\gamma_{\bar{U}}^{(1)} + \gamma_{H_S}^{(1)}) h_u^{H_S} + h_d^{H_S^\dagger} (\gamma_{\bar{D}}^{(1)} + \gamma_{H_S}^{(1)}) h_d^{H_S} \\
&\quad + h_u^{H_\lambda^\dagger} (\gamma_{\bar{U}}^{(1)} + \gamma_{H_\lambda}^{(1)}) h_u^{H_\lambda} + h_d^{H_\lambda^\dagger} (\gamma_{\bar{D}}^{(1)} + \gamma_{H_\lambda}^{(1)}) h_d^{H_\lambda})_{ij} \\
&\quad - \left( \frac{1}{30} g_1^2 + \frac{3}{2} g_2^2 + \frac{8}{3} g_3^2 \right) (\gamma_q^{(1)})_{ij} + \left( \frac{1}{30} b_1 g_1^4 + \frac{3}{2} b_2 g_2^4 + \frac{8}{3} b_3 g_3^4 \right) \delta_{ij},
\end{aligned} \tag{43}$$

$$\begin{aligned}
\gamma_U^{(2)} &= - \left( h_u^{H_\lambda^\dagger} (\gamma_U^{(1)} + \gamma_{H_\lambda}^{(1)}) h_u^{H_\lambda} + h_u^{H_S^\dagger} (\gamma_U^{(1)} + \gamma_{H_S}^{(1)}) h_u^{H_S} \right)_{(3,3)} \\
&\quad - \left( \frac{8}{15} g_1^2 + \frac{8}{3} g_3^2 \right) \gamma_U^{(1)} + \frac{8}{15} b_1 g_1^4 + \frac{8}{3} b_3 g_3^4,
\end{aligned} \tag{44}$$

$$\begin{aligned}
\gamma_D^{(2)} &= - \left( h_d^{H_\lambda^\dagger} (\gamma_D^{(1)} + \gamma_{H_\lambda}^{(1)}) h_d^{H_\lambda} + h_d^{H_S^\dagger} (\gamma_D^{(1)} + \gamma_{H_S}^{(1)}) h_d^{H_S} \right)_{(3,3)} \\
&\quad - \left( \frac{2}{15} g_1^2 + \frac{8}{3} g_3^2 \right) \gamma_D^{(1)} + \frac{2}{15} b_1 g_1^4 + \frac{8}{3} b_3 g_3^4,
\end{aligned} \tag{45}$$

$$\begin{aligned}
\gamma_Q^{(2)} &= - \left( h_u^{H_\lambda} (\gamma_{Q_u}^{(1)} + \gamma_{H_\lambda}^{(1)}) h_u^{H_\lambda^\dagger} + h_d^{H_\lambda} (\gamma_{Q_d}^{(1)} + \gamma_{H_\lambda}^{(1)}) h_d^{H_\lambda^\dagger} + h_u^{H_S} (\gamma_{Q_u}^{(1)} + \gamma_{H_S}^{(1)}) h_u^{H_S^\dagger} + h_d^{H_S} (\gamma_{Q_d}^{(1)} + \gamma_{H_S}^{(1)}) h_d^{H_S^\dagger} \right)_{(3,3)} \\
&\quad - \left( \frac{1}{30} g_1^2 + \frac{3}{2} g_2^2 + \frac{8}{3} g_3^2 \right) \gamma_Q^{(1)} + \frac{1}{30} b_1 g_1^4 + \frac{3}{2} b_2 g_2^4 + \frac{8}{3} b_3 g_3^4
\end{aligned} \tag{46}$$

For the leptons, the 2-loop anomalous dimensions can be obtained from the above expressions with the replacements  $u \rightarrow \nu$ ,  $d \rightarrow e$ ,  $q \rightarrow l$ , and inserting the gauge contributions adequately.

In this paper we have set the Yukawas for the first and second generation to zero. Nevertheless, they can be easily included once we replace the components  $x_f$ ,  $x'_c$ ,  $y_f$  and  $y'_c$  by three dimensional vectors, and thus the  $3 \times 3$  Yukawa matrices given in Eqs. (28-30) are enlarged to  $5 \times 5$  matrices.

The 1-loop and 2-loop anomalous dimensions for the Higgs scalars are,

(a) 1-loop anomalous dimensions,

$$\gamma_{H_1}^{(1)} = 3Tr[h_d^{H_1} h_d^{H_1^\dagger}] + Tr[h_e^{H_1} h_e^{H_1^\dagger}] + k_1^2 - \frac{3}{10} g_1^2 - \frac{3}{2} g_2^2, \tag{47}$$

$$\gamma_{H_2}^{(1)} = 3Tr[h_u^{H_1} h_u^{H_1^\dagger}] + Tr[h_\nu^{H_1} h_\nu^{H_1^\dagger}] + k_1^2 - \frac{3}{10} g_1^2 - \frac{3}{2} g_2^2, \tag{48}$$

$$\gamma_{H_S}^{(1)} = 6Tr[h_d^{H_S} h_d^{H_S^\dagger} + h_u^{H_S} h_u^{H_S^\dagger}] + 2Tr[h_e^{H_S} h_e^{H_S^\dagger} + h_\nu^{H_S} h_\nu^{H_S^\dagger}] + k_3^2, \tag{49}$$

$$\gamma_{H_\lambda}^{(1)} = 6Tr[h_d^{H_\lambda} h_d^{H_\lambda^\dagger} + h_u^{H_\lambda} h_u^{H_\lambda^\dagger}] + 2Tr[h_e^{H_\lambda} h_e^{H_\lambda^\dagger} + h_\nu^{H_\lambda} h_\nu^{H_\lambda^\dagger}] + 2k_1^2 + k_2^2 \tag{50}$$



(a) 2-loop contributions to the anomalous dimensions,

$$\begin{aligned}\gamma_{H_1}^{(2)} = & -3Tr[h_d^{H_1}\gamma_{Q_d}^{(1)}h_d^{H_1\dagger} + h_d^{H_1\dagger}\gamma_{\bar{D}}^{(1)}h_d^{H_1}] - Tr[h_e^{H_1}\gamma_{L_e}^{(1)}h_e^{H_1\dagger} + h_e^{H_1\dagger}\gamma_{\bar{E}}^{(1)}h_e^{H_1}] \\ & -k_1(\gamma_{H_1}^{(1)} + \gamma_{H_\lambda}^{(1)})k_1 - \left(\frac{3}{10}g_1^2 + \frac{3}{2}g_2^2\right)\gamma_{H_1}^{(1)} + \frac{3}{10}b_1g_1^4 + \frac{3}{2}b_2g_2^4, \quad (51)\end{aligned}$$

$$\begin{aligned}\gamma_{H_2}^{(2)} = & -3Tr[h_u^{H_1}\gamma_{Q_u}^{(1)}h_u^{H_1\dagger} + h_u^{H_1\dagger}\gamma_{\bar{U}}^{(1)}h_u^{H_1}] - Tr[h_\nu^{H_1}\gamma_{L_\nu}^{(1)}h_\nu^{H_1\dagger} + h_\nu^{H_1\dagger}\gamma_{\bar{\nu}}^{(1)}h_\nu^{H_1}] \\ & -k_1(\gamma_{H_2}^{(1)} + \gamma_{H_\lambda}^{(1)})k_1 - \left(\frac{3}{10}g_1^2 + \frac{3}{2}g_2^2\right)\gamma_{H_2}^{(1)} + \frac{3}{10}b_1g_1^4 + \frac{3}{2}b_2g_2^4, \quad (52)\end{aligned}$$

$$\begin{aligned}\gamma_{H_S}^{(2)} = & -6Tr[h_d^{H_S}\gamma_{Q_d}^{(1)}h_d^{H_S\dagger} + h_d^{H_S\dagger}\gamma_{\bar{D}}^{(1)}h_d^{H_S} + h_u^{H_S}\gamma_{Q_u}^{(1)}h_u^{H_S\dagger} + h_u^{H_S\dagger}\gamma_{\bar{U}}^{(1)}h_u^{H_S}] \\ & -2Tr[h_e^{H_S}\gamma_{L_e}^{(1)}h_e^{H_S\dagger} + h_e^{H_S\dagger}\gamma_{\bar{E}}^{(1)}h_e^{H_S} + h_\nu^{H_S}\gamma_{L_\nu}^{(1)}h_\nu^{H_S\dagger} + h_\nu^{H_S\dagger}\gamma_{\bar{\nu}}^{(1)}h_\nu^{H_S}] \\ & -k_3\gamma_{H_S}^{(1)}k_3 \\ \gamma_{H_\lambda}^{(2)} = & -6Tr[h_d^{H_\lambda}\gamma_{Q_d}^{(1)}h_d^{H_\lambda\dagger} + h_d^{H_\lambda\dagger}\gamma_{\bar{D}}^{(1)}h_d^{H_\lambda} + h_u^{H_\lambda}\gamma_{Q_u}^{(1)}h_u^{H_\lambda\dagger} + h_u^{H_\lambda\dagger}\gamma_{\bar{U}}^{(1)}h_u^{H_\lambda}] \\ & -2Tr[h_e^{H_\lambda}\gamma_{L_e}^{(1)}h_e^{H_\lambda\dagger} + h_e^{H_\lambda\dagger}\gamma_{\bar{E}}^{(1)}h_e^{H_\lambda} + h_\nu^{H_\lambda}\gamma_{L_\nu}^{(1)}h_\nu^{H_\lambda\dagger} + h_\nu^{H_\lambda\dagger}\gamma_{\bar{\nu}}^{(1)}h_\nu^{H_\lambda}] \\ & -k_3\gamma_{H_\lambda}^{(1)}k_3 \quad (53)\end{aligned}$$

## 5.2 Two-loop threshold effect formulae: step-function approximation.

We give here the two-loop coefficient for the gauge coupling RGE,  $b_{ij}$  and  $a_i^{(k)}$ , including the thresholds via a step-function,  $\theta_i$ , for the matter fields  $i = \tilde{w}$  wino,  $\tilde{g}$  gluino,  $\tilde{q}_L$ ,  $\tilde{u}_R$ ,  $\tilde{d}_R$ ,  $\tilde{l}_L$ ,  $\tilde{e}_R$ ,  $\tilde{h}$ ,  $H$ , and the vector-like superfields  $i = Q, L$ .  $n_f$  is the number of chiral generations, and  $n_V$  is the number of vector-like generations.

(a) Gauge contribution:

$$\begin{aligned}b_{11} = & n_f \left( \frac{19}{15} + (2 - \theta_{\tilde{w}}) \left( \frac{9}{100}\theta_{\tilde{l}_L} + \frac{18}{25}\theta_{\tilde{e}_R} + \frac{2}{75}\theta_{\tilde{d}_R} + \frac{1}{300}\theta_{\tilde{q}_L} + \frac{32}{75}\theta_{\tilde{u}_R} \right) \right) \\ & + \frac{9}{50} (1 + \theta_H + \theta_{\tilde{h}} (1 - \theta_{\tilde{w}})) \\ & + n_V (3 - \theta_{\tilde{w}}) \left( \frac{81}{100}\theta_L + \frac{137}{300}\theta_Q \right), \quad (54)\end{aligned}$$

$$\begin{aligned}
b_{12} = & n_f \left( \frac{3}{5} + (2 - \theta_{\tilde{w}}) \left( \frac{9}{20} \theta_{\tilde{l}_L} + \frac{3}{20} \theta_{\tilde{q}_L} \right) \right) \\
& + \frac{9}{10} (1 + \theta_H + \theta_{\tilde{h}} (1 - \theta_{\tilde{w}})) \\
& + n_V (3 - \theta_{\tilde{w}}) \left( \frac{9}{20} \theta_L + \frac{3}{20} \theta_Q \right), \tag{55}
\end{aligned}$$

$$\begin{aligned}
b_{13} = & n_f \left( \frac{44}{15} + (2 - \theta_{\tilde{g}}) \left( \frac{4}{15} \theta_{\tilde{q}_L} + \frac{6}{15} \theta_{\tilde{d}_R} + \frac{32}{15} \theta_{\tilde{u}_R} \right) \right) \\
& + n_V (3 - \theta_{\tilde{g}}) \frac{44}{15} \theta_Q, \tag{56}
\end{aligned}$$

$$\begin{aligned}
b_{21} = & n_f \left( \frac{1}{5} + (2 - \theta_{\tilde{w}}) \left( \frac{3}{20} \theta_{\tilde{l}_L} + \frac{1}{20} \theta_{\tilde{q}_L} \right) \right) \\
& + \frac{3}{10} (1 + \theta_H + \theta_{\tilde{h}} (1 - \theta_{\tilde{w}})) \\
& + n_V (3 - \theta_{\tilde{w}}) \left( \frac{3}{20} \theta_L + \frac{1}{20} \theta_Q \right), \tag{57}
\end{aligned}$$

$$\begin{aligned}
b_{22} = & -\frac{136}{3} + \frac{64}{3} \theta_{\tilde{w}} + n_f \left( \frac{49}{3} + (26 - 33 \theta_{\tilde{w}}) \left( \frac{1}{12} \theta_{\tilde{l}_L} + \frac{1}{4} \theta_{\tilde{q}_L} \right) \right) \\
& + \left( \frac{13}{6} + \frac{13}{6} \theta_H + \theta_{\tilde{h}} \left( \frac{49}{6} - \frac{11}{2} \theta_{\tilde{w}} \right) \right) \\
& + n_V (25 - 11 \theta_{\tilde{w}}) \left( \frac{1}{4} \theta_L + \frac{3}{4} \theta_Q \right), \tag{58}
\end{aligned}$$

$$\begin{aligned}
b_{23} = & n_f (4 + 4 (2 - \theta_{\tilde{g}}) \theta_{\tilde{q}_L}) \\
& + n_V 4 (3 - \theta_{\tilde{g}}) \theta_Q, \tag{59}
\end{aligned}$$

$$\begin{aligned}
b_{31} = & n_f \left( \frac{11}{30} + (2 - \theta_{\tilde{g}}) \left( \frac{1}{30} \theta_{\tilde{q}_L} + \frac{1}{15} \theta_{\tilde{d}_R} + \frac{4}{15} \theta_{\tilde{u}_R} \right) \right) \\
& + n_V \frac{11}{30} (3 - \theta_{\tilde{g}}) \theta_Q, \tag{60}
\end{aligned}$$

$$\begin{aligned}
b_{32} = & n_f \left( \frac{3}{2} + \frac{3}{2} (2 - \theta_{\tilde{g}}) \theta_{\tilde{q}_L} \right) \\
& + n_V \frac{3}{2} (3 - \theta_{\tilde{g}}) \theta_Q, \tag{61}
\end{aligned}$$

$$\begin{aligned}
b_{33} = & -102 + 48 \theta_{\tilde{g}} + n_f \left( \frac{76}{3} + \left( \frac{11}{3} - \frac{13}{3} \theta_{\tilde{g}} \right) (2 \theta_{\tilde{q}_L} + \theta_{\tilde{d}_R} + \theta_{\tilde{u}_R}) \right) \\
& + n_V \left( 40 - \frac{52}{3} \theta_{\tilde{g}} \right) \theta_Q \tag{62}
\end{aligned}$$

(b) Yukawa contribution

To write down the coefficients  $a_i^{(k)}$ , let us define  $\hat{\gamma}_j^{(1)}$  to be the anomalous dimensions without the gauge contributions:

$$\begin{aligned}
\sum_k a_1^{(k)} = & \frac{6}{5} \left( \frac{4}{3} (Tr \hat{\gamma}_{\tilde{u}}^{(1)} + \hat{\gamma}_U^{(1)}) + \frac{1}{3} (Tr \hat{\gamma}_{\tilde{d}}^{(1)} + \hat{\gamma}_D^{(1)}) + \frac{1}{6} (Tr \hat{\gamma}_q^{(1)} + \hat{\gamma}_Q^{(1)}) + Tr \hat{\gamma}_e^{(1)} + \hat{\gamma}_E^{(1)} + \frac{1}{2} (Tr \hat{\gamma}_l^{(1)} + \hat{\gamma}_L^{(1)}) \right. \\
& \left. + \frac{1}{2} (\hat{\gamma}_{H_1}^{(1)} + \hat{\gamma}_{H_2}^{(1)}) \right), \tag{63}
\end{aligned}$$

$$\sum_k a_2^{(k)} = 3 \left( \text{Tr} \hat{\gamma}_q^{(1)} + \hat{\gamma}_{\bar{Q}}^{(1)} \right) + \text{Tr} \hat{\gamma}_l^{(1)} + \hat{\gamma}_L^{(1)} + \hat{\gamma}_{H_1}^{(1)} + \hat{\gamma}_{H_2}^{(1)}, \quad (64)$$

$$\sum_k a_3^{(k)} = \text{Tr} \hat{\gamma}_{\bar{u}}^{(1)} + \text{Tr} \hat{\gamma}_{\bar{d}}^{(1)} + \hat{\gamma}_U^{(1)} + \hat{\gamma}_D^{(1)} + 2 \left( \text{Tr} \hat{\gamma}_q^{(1)} + \hat{\gamma}_{\bar{Q}}^{(1)} \right). \quad (65)$$

The vector-like superfields are decoupled at their respective scales ( $M_Q$ ,  $M_L$ ) rotating the Yukawa matrices such that,

$$h_u^{H_2}(\mu < M_Q) = \begin{pmatrix} h_t(\mu) & 0 & 0 \\ 0 & 0 & 0 \\ 0 & 0 & 0 \end{pmatrix}, \quad (66)$$

$$h_u^{H_S}(\mu < M_Q) = h_u^{H_\lambda}(\mu < M_Q) = 0, \quad (67)$$

$$h_d^{H_1}(\mu < M_Q) = \begin{pmatrix} h_b(\mu) & 0 & 0 \\ 0 & 0 & 0 \\ 0 & 0 & 0 \end{pmatrix}, \quad (68)$$

$$h_d^{H_S}(\mu < M_Q) = h_d^{H_\lambda}(\mu < M_Q) = 0, \quad (69)$$

$$h_e^{H_1}(\mu < M_L) = \begin{pmatrix} h_\tau(\mu) & 0 & 0 \\ 0 & 0 & 0 \\ 0 & 0 & 0 \end{pmatrix}, \quad (70)$$

$$h_e^{H_S}(\mu < M_L) = h_e^{H_\lambda}(\mu < M_L) = 0, \quad (71)$$

with the boundary conditions given in Eq. (5). This ensures the decoupling of the vector-like contributions in both the gauge coupling and the Yukawa coupling evolutions.

## References

- [1] K. S. Babu and J. C. Pati, Phys. Lett **B384**, 140 (1996)
- [2] P. Langacker and N. Polonsky, Phys. Rev. **D52**, 3081 (1995)
- [3] P. Ginsparg, Phys. Lett. **B 197**, 139 (1987); V. S. Kaplenovsky, Nucl. Phys. **B 307**, 145 (1988); erratum: ibid. **B442**, 461 (1995)
- [4] K. S. Babu, J. C. Pati and H. Stremnitzer, Phys. Rev. Lett **67**, 1688 (1991); Phys. Rev. **D 51**, 2451 (1995)
- [5] K.S. Babu, K. Choi, J.C. Pati and X. Zhang, Phys. Lett. **B333** 364 (1994)
- [6] M. Bastero-Gil and J. Perez-Mercader, Nucl. Phys. **B450**, 21 (1995)
- [7] J. Bagger, K. Machev and D. Pierce, Phys. Lett. **348**, 443 (1995)
- [8] C. Kolda, J. March-Russell, Phys. Rev. **D55**, 4252 (1997)
- [9] P. Fayet, Nucl. Phys. **B90**, 104 (1975); H. P. Nilles, M. Srednicki, and D. Wyler, Phys. Lett. **120 B**, 346 (1983); L. Durand and J. L. Lopez, Phys. Lett. **B217**, 46 (1989); M. Drees, Int. J. Mod. Phys. **A 4**, 3645 (1989).

- [10] J. M. Frere, D. R. T. Jones and S. Raby, Nucl. Phys. **B222**, 11 (1983); J.-P. Derendinger and C. A. Savoy, *ibid* **B237**, 307 (1984)
- [11] J. Ellis, J. Gunion, H. Haber, L. Roszkowski and F. Zwirner, Phys. Rev. **D39**, 844 (1989); U. Ellwanger, M. Rausch de Traubenberg and C. A. Savoy, Phys. Lett. **B315** (1993) 331; T. Elliott, S. F. King and P. L. White, Phys. Lett. **B305** (1993) 71; *ibid* **314** (1993) 56; Phys. Rev. **D49** (1994) 2435; U. Ellwanger, M. Rausch de Traubenberg and C. A. Savoy, Z. Phys. **C 67** (1995) 665; S. F. King and P. L. White, Phys. Rev. **D52**, 4183 (1995)
- [12] L. Alvarez-Gaumé, J. Polchinski and M. Wise, Nucl. Phys. **B221** (1983) 495; M. Claudson, L. J. Hall and I. Hinchliffe, Nucl. Phys. **B 228** (1983) 501; C. Kounnas, A. B. Lahanas, D. V. Nanopoulos and M. Quirós, Nucl. Phys. **B236** (1984) 438; M. Drees, M. Gück and K. Grassie, Phys. Lett. **157** (1985) 164; J. F. Gunion, H. E. Haber and M. Sher, Nucl Phys. **306** (1988) 1; H. Komatsu, Phys. Lett. **215** (1988) 323.
- [13] J. A. Casas, A. Lleyda and C. Muñoz, Nucl. Phys. **B471** (1996) 1; Phys. Lett. **B389** (1996) 305; S. A. Abel and C. A. Savoy, Phys. Lett **444** (1998) 119; *ibid* **B444** (1998) 427.
- [14] J. Ellis, G. Ridolfi and F. Zwirner, Phys. Lett. **257** (1991) 83; *ibid* **B262** (1991) 477; A. Brignole, J. Ellis, G. Ridolfi and F. Zwirner, *ibid* **B271** (1991), 123.
- [15] See for example S. F. King and P. L. White in Ref. [11], and references therein.
- [16] R. Hempfling, Phys. Lett **B351**, 206 (1995); B. Brahmachari, U. Sarkar and K. Sridhar, Mod. Phys. Lett **A8**, 3349 (1993); L. Maiani, G. Parisi and R. Petronzio, Nucl. Phys. **B136**, 115 (1978).
- [17] K. Inoue et al, Prog. Theor. Phys. **68**, 927, (1982); *ibid* **67**, 1889 (1982). J. E. Bjorkman and D. R. T. Jones, Nucl. Phys. **B259**, 533 (1985).
- [18] P. West, “*Introduction to supersymmetry and supergravity*” (World Scientific, Singapore, 1990) page 179.